Polyhedron 33 (2012) 127–136

Contents lists available at SciVerse ScienceDirect

Polyhedron

journal homepage: www.elsevier.com/locate/poly

Structure diversity of a series of new coordination polymers based on a C_3-symmetric tridentate ligand with rosette architecture

Yang Zhang [a], Qian Wang [a], Yuan-Jing Xiao [a], Jie Han [b], Xiao-Li Zhao [a],*

[a] Shanghai Key Laboratory of Green Chemistry and Chemical Processes, Department of Chemistry, East China Normal University, 3663 North Zhongshan Road, Shanghai 200062, PR China
[b] School of Science & Technology, The Open University of Hong Kong, Kowloon, Hong Kong, PR China

ARTICLE INFO

Article history:
Received 5 August 2011
Accepted 10 November 2011
Available online 22 November 2011

Keywords:
Rosette
C_3-symmetric
Coordination polymers

ABSTRACT

4,4′,4″-[1,3,5-Benzenetriyltris(carbonylimino)]trisbenzoic acid (H_3L), a C_3-symmetric ligand, was found to self-assemble into an interesting core-rosette structure driven by intermolecular hydrogen-bonding interactions. Reactions of this ligand with Zn^{2+}, Co^{2+} and Cd^{2+} under solvothermal conditions resulted in the formation of four new coordination polymers with interesting structural motifs: $[Zn_2(L)(OH)(H_2O)(DMF)]\cdot DMF\cdot H_2O$ (**1**), $[Co_3(L)_2(DMF)(H_2O)]\cdot DMF\cdot 3CH_3OH$ (**2**), $[Co_{1.5}(L)(H_2O)(DMF)]\cdot DMF$ (**3**), and $[Cd_{1.5}(L)(H_2O)(DMF)]\cdot DMF$ (**4**). Single-crystal structural analysis revealed that complex **1** exhibits a rare example of twofold interpenetrating two-dimensional CdI_2-type structure with tetranuclear $Zn_4(\mu_3\text{-}OH)_2(COO)_6(H_2O)(DMF)$ serving as secondary building unit (SBU), whereas in **2**, the μ_3-oxo-tricobalt basic carboxylate SBUs are connected by L^{3-} ligands, leading to a twofold interpenetrating three-dimensional (3,6)-net framework. The isomorphous complexes **3** and **4** each has a (4,4)-grid layered architecture in which the SBU is a linear Co_3/Cd_3 cluster. The four coordination polymers were all further characterized by IR, thermogravimetric and powder X-ray diffraction (PXRD).

1. Introduction

Coordination polymers (CPs), which are obtained by assembling metal ions with bridging organic ligands via coordination bonds associated with hydrogen bonds, π–π stacking and other supramolecular interactions, have been extensively explored because of their wide applications in catalysis [1], magnetism [2], drug delivery [3], gas storage and adsorptive separation [4]. The specific properties of CPs arise essentially from a judicious choice of metal ions or clusters and deliberately designed organic linkers with specific configuration and functional groups. Thus, by careful selection of metal ions, organic ligands and synthetic strategies, CPs with specific structures and functionalities could be constructed. Two types of strategies are currently employed in the construction of functionalized CPs: namely, (1) immobilization of coordinatively unsaturated (open) metal sites (OMS) in a defined CP, and (2) introduction of organic functional groups to provide guest-accessible functional organic sites (FOS). Numerous studies on the use of OMS as Lewis acid catalysts and gas adsorption materials have been reported in past few years [5]. However, research on the introduction of FOS in CPs are less documented, possibly due to the difficulty encountered in producing the guest-accessible FOS on the pore surfaces as those organic groups tend to interact with metal ions, which resulted in the blocking of the FOS within the CPs [6].

Recently, our group has focused on developing and designing ligands having amide functionality. In this report, we employed a C_3-symmetric tridentate bridging ligand, 4,4′,4″-[1,3,5-benzenetriyltris(carbonylimino)]trisbenzoic acid (H_3L, Chart 1) to build CPs. There are multiple reasons for exploring H_3L. First, the combination of threefold symmetric carboxylic acid and amide units makes H_3L itself an ideal building block in the field of crystal engineering; Second, the tridentate bridging carboxylate ligands have exhibited great potential for the generation of supramolecular cages or multi-dimensional porous CPs, which thus offers possibilities for the development of stable porous systems that can accommodate small molecular guests or catalysts, for instance, Lah and co-workers synthesized a series of metal–organic polyhedra exhibiting interesting structures and high surface areas using tritopic ligand [7]. It was also well documented by Zhou that three-dimensional porous CPs showing excellent gas absorption properties could be obtained via the incorporation of C_3-symmetric ligands [8]. Furthermore, the amide group is a fascinating functional group as it possesses both hydrogen-bonding donor and acceptor sites with the –NH moiety acts as an electron acceptor and the –C=O group acts as an electron donor. With this special structural property, amide group has been extensively employed in the construction of porous CPs with guest-accessible functional

---

* Corresponding author. Fax: +86 21 62233179.
E-mail address: xlzhao@chem.ecnu.edu.cn (X.-L. Zhao).

0277-5387/$ - see front matter © 2011 Elsevier Ltd. All rights reserved.
doi:10.1016/j.poly.2011.11.010

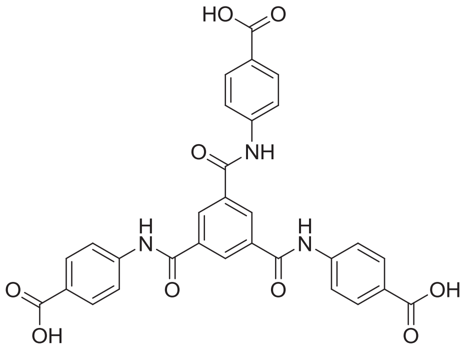

Chart 1. Structure of the C_3-symmetric tricarboxylic ligand H_3L.

organic sites for selective sorption and/or catalysis inside the channels. Recently, Kitagawa reported a three-dimensional porous CPs functionalized with amide group displaying selective gas sorption and catalytic properties [9]. Zaworotko and co-workers demonstrated that decoration of a porous architecture with polar acrylamide groups can significantly enhance the CO_2 binding ability [10].

We report herein the solvothermal syntheses and structure characterizations of a family of coordination polymers based on C_3-symmetric ligand 4,4′,4″-[1,3,5-benzenetriyltris(carbonylimino)]trisbenzoic acid (H_3L): $[Zn_2(L)(OH)(H_2O)(DMF)]\cdot DMF\cdot H_2O$ (**1**), $[Co_3(L)_2(DMF)(H_2O)]\cdot DMF\cdot 3CH_3OH$ (**2**), $[Co_{1.5}(L)(H_2O)(DMF)]\cdot DMF$ (**3**), and $[Cd_{1.5}(L)(H_2O)(DMF)]\cdot DMF$ (**4**). The supramolecular assembly of H_3L under solvothermal condition will also be presented.

2. Experimental

2.1. Materials and physical measurements

All chemicals and reagents of analytical grade were commercially purchased and used without further purification. NMR spectra were obtained using a Bruker Avance III 400 M instrument. Elemental analyses were determined on a Vario ELIII Elemental Analyzer. FT-IR spectra were recorded in the range 500–4000 cm^{-1} using KBr pellets on a Nicolet NEXUS 670 spectrophotometer. Thermogravimetric analyses (TGA) was carried out on a Mettler Toledo TGA/SDTA851 instrument from room temperature to 800 °C under N_2 atmosphere at a heating rate of 10 °C min^{-1}. Powder X-ray diffraction (PXRD) data were recorded using a Rigaku (D/Max-Ultima IV) diffractometer equipped with Cu Kα radiation, with a step size of 1° in 2θ angle. Simulated PXRD patterns were calculated with the Mercury program using the single crystal data.

2.2. Synthesis of 4,4′,4″-[1,3,5-benzenetriyltris(carbonylimino)] trisbenzoic acid (H_3L)

Methyl 4-aminobenzoate and 1,3,5-benzenetricarboxylic acid chloride were synthesized using the literature method [11].

2.2.1. Preparation of 4,4′,4″-[1,3,5-benzenetriyltris(carbonlimino)]trisbenzoic acid methyl ester

A solution of methyl 4-aminobenzoate (7.2 g, 48 mmol), 1,3,5-benzenetricarboxylic acid chloride (3.65 g, 13.6 mmol), and K_2CO_3 (6.63 g, 49 mmol) in 100 mL acetone was stirred for 12 h at 80 °C. After filtration, the resulted white precipitate was washed with water and then air-dried (8.45 g, yield: 87.3%). ^1H NMR (300 MHz, DMSO-d_6): δ = 3.848 (s, 9 H), 8.001(s, 12H), 8.752(s, 3H), 10.916(s, 3H) ppm.

2.2.2. Preparation of 4,4′,4″-[1,3,5-benzenetriyltris(carbonylimino)] trisbenzoic acid

4 M NaOH aqueous solution (12.2 mL) was added slowly to 4,4′,4″-[1,3,5-benzenetriyltris(canbonlimino)]trisbenzoic acid methyl ester (8.45 g, 13.8 mmol) suspended in DMF (100 mL). The mixture was stirred under reflux overnight and then filtered. The resulted precipitate was washed with acetonitrile, acetone and then added to aqueous solution (50 mL) of NaOH (0.028 g) to carry out the second hydrolysis. The mixture was stirred at 90 °C for 10 h. Dilute HCl (1 M) was added to the remaining aqueous solution until pH <1. After filtration, the solid was washed with water and acetone to give H_3L (6.06 g, yield: 67.3%). *Anal.* Calc. for $C_{30}H_{21}N_3O_9\cdot 3H_2O$: C, 57.97; H, 4.38; N, 6.76. Found: C, 58.57; H, 4.63; N, 6.87%. Melting point: 364 °C. ^1H NMR (400 MHz, DMSO-d_6): δ 7.978(s, 12H), 8.752(s, 3H), 10.893(s, 3H), 12.809 (s, 3H). ^{13}C NMR (100 MHz, DMSO-d_6): δ 167.38, 165.27, 165.18, 143.45, 135.67, 130.81, 126.35, 120.13, 120.04. IR (KBr, cm^{-1}): 3323(m), 3190(m), 1697(s), 1600(s), 1531(m), 1408(s), 1249(s), 1174(w), 1116(w), 1014(w), 954(w), 853(w).

2.2.3. Crystals of 4,4′,4″-[1,3,5-benzenetriyltris(carbonylimino)] trisbenzoic acid (H_3L)

H_3L is insoluble in water at room temperature but quite soluble in many organic solvents such as dimethylformamide (DMF), dimethylacetamide (DMA) and dimethyl sulfoxide (DMSO). However, it is quite difficult to get single crystal suitable for X-ray diffraction via evaporation or diffusion. Attempts to assemble the sodium salt of H_3L with metal salt failed, but we harvested the single crystals of H_3L as a result. It was entirely serendipitous. A mixture of Na_3L (19 mg, 0.03 mmol) and $ZnCl_2$ (6.13 mg, 0.045 mmol) was dissolved in H_2O (5 mL) and CH_3CN (8 mL) and then placed in a 20 mL Teflon-lined stainless steel reaction vessel. After the addition of three drops of HF, the reaction vessel was placed in an oven at 180 °C for 48 h and then cooled to room temperature (cooling rate: 0.1 °C/min). The obtained small colorless square dipyramidal crystals were washed with CH_3CN several times to produce pure sample.

2.3. Synthesis of $[Zn_2(L)(OH)(H_2O)(DMF)]\cdot DMF\cdot H_2O$ (**1**)

A mixture of H_3L (13.0 mg, 0.023 mmol) and $Zn(NO_3)_2\cdot 6H_2O$ (34.1 mg, 0.115 mmol) in 2 mL DMF/H_2O (1:1) was placed in a 20 mL Teflon-lined stainless steel reaction vessel and subjected to solvothermal condition at 120 °C for 30 h and then cooled to room temperature (cooling rate: 0.1 °C/min). The resulted colorless block crystals were washed with DMF to give **1** (10.04 mg, yield 50% based on H_3L). *Anal.* Calc.: C, 48.34; H, 3.83; N, 7.83. Found: C, 48.52; H, 4.11; N, 7.57%. IR (KBr, cm^{-1}): 3280(m), 3082(m), 1653(s), 1605(vs), 1559(m), 1522(vs), 1386(s), 1251(s), 1177(w), 1104(w), 1014(w), 862(w), 783(w), 732(w), 696(w).

2.4. Synthesis of $[Co_3(L)_2(DMF)(H_2O)]\cdot DMF\cdot 3CH_3OH$ (**2**)

H_3L (65.0 mg, 0.115 mmol) and $CoCl_2\cdot 6H_2O$ (27.2 mg, 0.115 mmol) in DMF/CH_3OH media (4:3, 7 mL) were sealed in a 20 mL Teflon-lined stainless steel reaction vessel and subjected to solvothermal condition at 150 °C for 36 h after ultrasonic treatment. The purple crystals obtained were washed with DMF to give **2** (31.49 mg, yield 26% based on $CoCl_2$). IR (KBr, cm^{-1}): 3272(m), 1650(s), 1602(vs), 1524(vs), 1387(s), 1252(s), 1177(w), 1100(w), 861(w), 782(w), 729(w), 698(w).

2.5. Synthesis of $[Co_{1.5}(L)(H_2O)(DMF)]\cdot DMF$ (**3**)

H_3L (13.0 mg, 0.023 mmol) and $Co(NO_3)_2\cdot 6H_2O$ (33.3 mg, 0.115 mmol) in a mixture of DMF/H_2O (1:5, 3 mL) were sealed in a 20 mL Teflon-lined stainless steel reaction vessel and subjected to solvothermal condition at 120 °C for 40 h before cooled to room temperature. The purple crystals obtained were washed with DMF to give **3** (10.32 mg, yield 55% based on H_3L). *Anal.* Calc.: C, 52.92; H, 3.82; N, 8.57. Found: C, 52.40; H, 4.23; N, 8.27%. IR (KBr, cm^{-1}): 3280(m), 3082(m), 1650(s), 1609(vs), 1556(m), 1532(vs), 1388(s), 1253(s), 1187(w), 1102(w), 1016(w), 883(w), 785(w), 733(w), 696(w).

2.6. Synthesis of $[Cd_{1.5}(L)(H_2O)(DMF)]\cdot DMF$ (**4**)

When the procedure for **3** was repeated with $Cd(NO_3)_2\cdot 4H_2O$ instead of $Co(NO_3)_2\cdot 6H_2O$, colorless needle-shaped crystals of **4** were obtained in 56% based on H_3L (11.57 mg). *Anal.* Calc.: C, 48.19; H, 3.48; N, 7.80. Found: C, 47.83; H, 4.82; N, 7.53%. IR (KBr, cm^{-1}): 3320(m), 1660(s), 1609(vs), 1556(m), 1530(vs), 1388(s), 1232(s), 1200(w), 1102(w), 1010(w), 860(w), 779(w), 733(w), 696(w).

2.7. Crystal structures determination and refinement

Single-crystal X-ray diffraction data were collected on a Bruker SMART ApexII diffractometer equipped with graphite-monochromatic Mo Kα radiation ($\lambda = 0.71073$ Å) operating at 50 kV and 40 MA. Crystals were coated with paratone oil and the diffraction data collected at 173 K cooled in a nitrogen stream. Frames were collected with 0.6° intervals in φ and ω for 30 s per frame such that a hemisphere of data was collected. Raw data collection and refinement were done using SMART. Data reduction was performed using SAINT+ [12]. An empirical absorption correction was applied using the SADABS program [13]. The structures were solved by direct method and refined by full-matrix least-squares on F^2 with anisotropic displacement using SHELX-97 [14]. Non-hydrogen atoms were refined with anisotropic displacement parameters during the final cycles. All the hydrogen atoms attached to carbon atoms were placed in calculated positions and refined using the riding model. PLATON/SQUEEZE [15] was employed to calculate the diffraction contribution of the solvent molecules in complex **2** and, thereby, to produce a set of solvent-free diffraction intensities; structure was then refined again using the data generated. Details of the data collection and the refinement of the structures are summarized in Table 1.

3. Results and discussion

3.1. Crystal structures

3.1.1. 4,4′,4″-[1,3,5-Benzenetriyltris(carbonylimino)]trisbenzoic acid (H_3L)

Design and assembly of aesthetic supramolecular rosette motifs have drawn much current attention in the field of crystal engineering [16]. Among many methods used for organizing rosette structures, self-assembly based on hydrogen-bonding is found to be especially effective. A dominant strategy to construct organic rosettes is to employ C_3-symmetric molecular building blocks with suitable shapes and sizes such that their donor and acceptor sites are perfectly matched [17].

4,4′,4″-[1,3,5-Benzenetriyltris(carbonylimino)]trisbenzoic acid (H_3L), which combines the threefold symmetric carboxylic acid and amide units, is an ideal molecular building block for engineering rosette structures. Single-crystal X-ray analysis revealed that H_3L contains the desired rosette structure and crystallizes in hexagonal space group $P6_5$. As shown in Fig. 1a, the trigonal angles of the H_3L are respectively 119.65(6)°, 119.89(6)° and 120.46(6)°, suggesting a C_3-symmetry of the ligand (H_3L), which is in good agreement with our initial design (Table 2). Planar rosette-layered architecture was formed via intermolecular hydrogen-bonding interactions between the amide and carboxylic acid groups. Two types of hydrogen bonds (six N–H···O and six O–H···O hydrogen bonds) between each central H_3L and its six neighboring H_3L molecules constitute a honeycomb grid (shown in Fig. 1b). By simplifying H_3L as a triangle, the triangle in light gray surrounded by six deep gray ones serves as a core of the rosette, and such an arrangement could also be named as a core-rosette.

All molecules arranged in the layer-type lattice are coplanar, and the distance between adjacent layers of the two-dimensional honeycomb grids is 2.9 Å. It should be noticed that the two adjacent core-rosette layers do not stack on top of each other, but are reversed from each other with a rotational relationship of about 180° (Fig. 2). The significant reversal and staggered packing of the rosettes may be caused by the formation of stable lattice via optimization of the packing interactions [18].

3.1.2. Crystal structure of $[Zn_2(L)(OH)(H_2O)(DMF)]\cdot DMF\cdot H_2O$ (**1**)

Solvothermal reaction of H_3L with $Zn(NO_3)_2\cdot 6H_2O$ in mixed solvent of DMF/H_2O at 120 °C gave crystalline product **1**. Structure

Table 1
Crystal data and structure refinement for H_3L and complexes **1**–**4**.

Compound	H_3L	**1**	**2**	**3**	**4**
Empirical formula	$C_{30}H_{21}N_3O_9$	$C_{36}H_{18}N_5O_{14}Zn_2$	$C_{64}H_{42}N_7O_{21}Co_3$	$C_{36}H_{32}N_5O_{12}Co_{1.5}$	$C_{36}H_{32}N_5O_{12}Cd_{1.5}$
Formula weight	567.50	875.29	1421.84	815.06	895.27
Crystal system	Hexagonal	Triclinic	Monoclinic	Triclinic	Triclinic
Space group	$P6_5$	$P\bar{1}$	$P2(1)/n$	$P\bar{1}$	$P\bar{1}$
Unit cell dimensions					
a (Å)	15.0699(6)	11.5311(3)	13.8773(6)	10.7005(7)	10.7208(4)
b (Å)	15.0699(6)	12.8202(3)	21.6080(8)	12.7457(9)	12.7765(4)
c (Å)	18.9408(9)	14.8449(3)	34.922 (1)	14.312 (1)	14.3962(5)
α (°)	90.00	82.8740	90	84.334	82.741
β (°)	90.00	74.0740	96.24(1)	74.103	74.849
γ (°)	120.00	65.1980	90	65.560	65.910
V (Å^3)	3725.2(3)	1915.89(8)	10409.8(7)	1708.9(2)	1737.6(1)
Z	6	2	4	2	2
ρ_{calc} (mg cm^{-3})	1.518	1.517	0.907	1.584	1.711
μ (mm^{-1})	0.114	1.326	0.523	0.812	1.000
$F(000)$	1764	882	2896	839	902
θ Range (°)	1.56–25.01	1.75–25.01	1.11–25.01	1.76–25.01	1.47–25.01
R_{int}	0.0314	0.0164	0.0764	0.0441	0.0286
Final R indices [$I > 2\sigma(I)$]	$R_1 = 0.0498$, $wR_2 = 0.1509$	$R_1 = 0.0501$, $wR_2 = 0.1429$	$R_1 = 0.0844$, $wR_2 = 0.2302$	$R_1 = 0.0542$, $wR_2 = 0.1489$	$R_1 = 0.0322$, $wR_2 = 0.0758$
R indices (all data)	$R_1 = 0.0546$, $wR_2 = 0.1569$	$R_1 = 0.0537$, $wR_2 = 0.1467$	$R_1 = 0.1185$, $wR_2 = 0.2495$	$R_1 = 0.0771$, $wR_2 = 0.1666$	$R_1 = 0.0435$, $wR_2 = 0.0827$

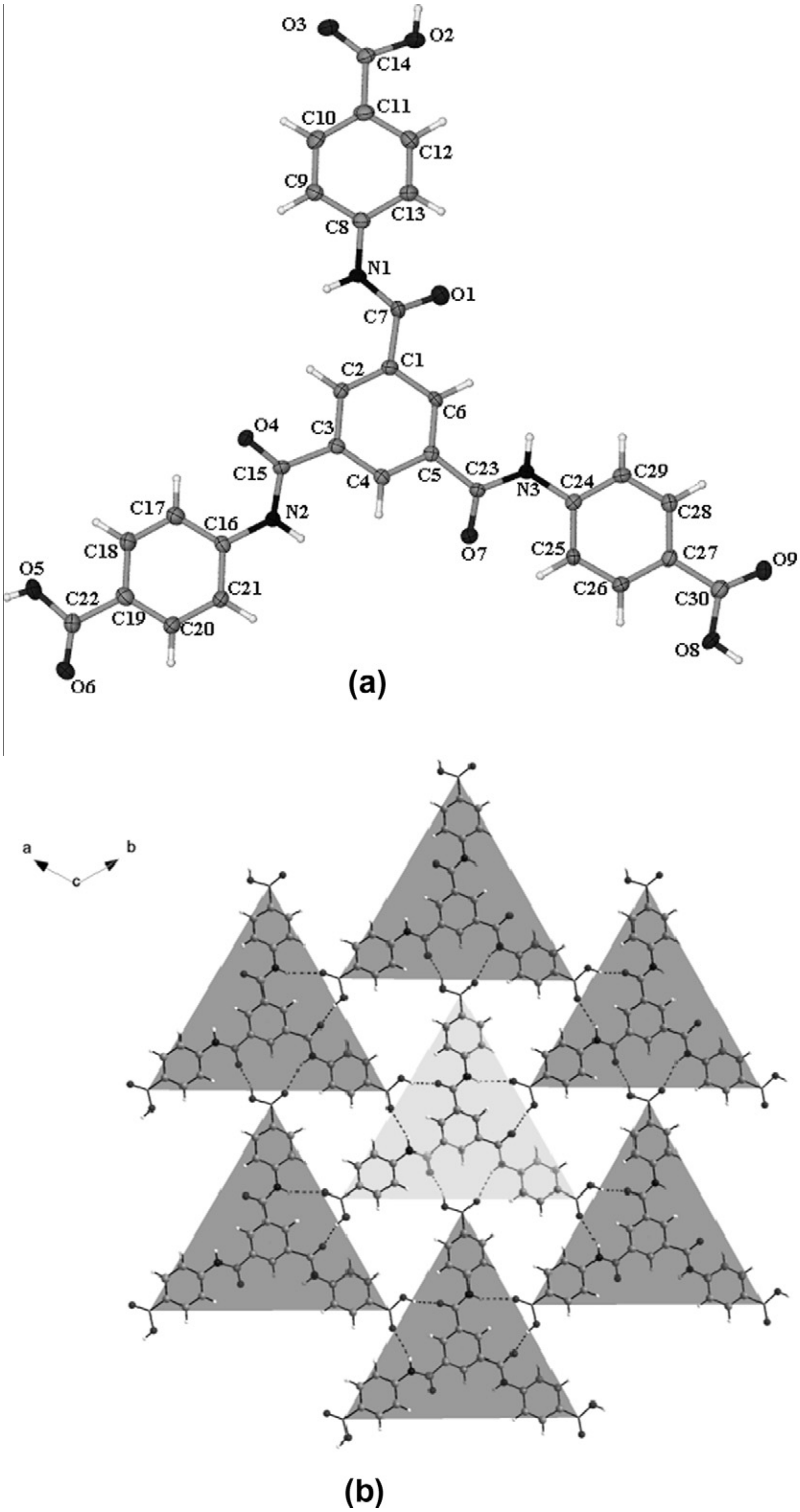

Fig. 1. Ball-and-Stick showing (a) the crystal structure of H_3L with thermal ellipsoids drawn at 50% probability. The trigonal angle was measured from the C atom of the carboxylic acid group to the dummy atom, the center of the central phenyl ring of the ligand, to another C atom of a neighboring carboxylic group in the ligand. (b) Two-dimensional core-rosette architecture of H_3L viewed along the *c* direction.

analysis revealed a twofold interpenetrating architecture with centrosymmetric tetranuclear $Zn_4(\mu_3\text{-OH})_2(COO)_6(H_2O)(DMF)$ serving as the basic secondary building unit (SBU). As depicted in Fig. 3a, Zn1 is six-coordinated with a distorted octahedral geometry involving two oxygen atoms from two carboxylate groups, two μ_3-OH, one aqua ligand (O3W) and one oxygen atom (O11) from disordered DMF [average Zn–O = 2.077(3) Å]. Zn2 adopts a tetrahedral coordination environment and is coordinated by three oxygen atoms from three independent carboxylate groups and one μ_3-OH [average Zn–O = 1.968(3) Å]. The four Zn(II) ions are located at four vertices with the Zn···Zn separations in the ranges of 3.0830(8)–3.1422(2) Å, and the bridging Zn–O–Zn angles of

Table 2
The trigonal angles (°) for the four ligands in H_3L and complexes **1**–**4**.

H_3L	119.65(6)	119.89(6)	120.46(6)
1	92.21(6)	132.98(6)	124.03(6)
2	117.04(6)	120.44(6)	120.19(6)
	120.40(7)	113.62(8)	117.04(7)
3	92.26(6)	112.43(6)	145.04(7)
4	144.12(5)	112.88(5)	92.81(5)

96.8(1)–128.5(1)° are all in good accordance with the reported complexes [19]. The linkages between Zn1 and Zn2, Zn1a and Zn2a are achieved by two carboxylate groups and one μ_3-OH, while in the cases of Zn2 and Zn1a, Zn1 and Zn2a, the centers are connected by one μ_3-OH. This kind of tetranuclear SBU $Zn_4(\mu_3\text{-}OH)_2(COO)_6(H_2O)(DMF)$ containing co-existence of four- and six-coordinated Zn(II) is quite different from previously reported Zn_4O basic carboxylate $M_4O(CO_2)_6$ SBU [20].

The four Zn(II) ions bridged by the hydroxyl and carboxylate oxygen atoms serving as SBU are jointly coordinated by six L^{3-} anions to generate an infinite layer (Fig. 3b). A better view of this interesting framework could be achieved by the application of a topological approach via reducing the multi-dimensional structures to simple node and connection nets. The L^{3-} ligand can be viewed as a three-connected node, and the $Zn_4(\mu_3\text{-}OH)_2(COO)_6(H_2O)(DMF)$ unit as a six-connected node, respectively. The whole structure can thus be simplified as a (3,6)-connected two-dimensional net with grilles (10.742 × 8.108 Å) occupied by DMF and

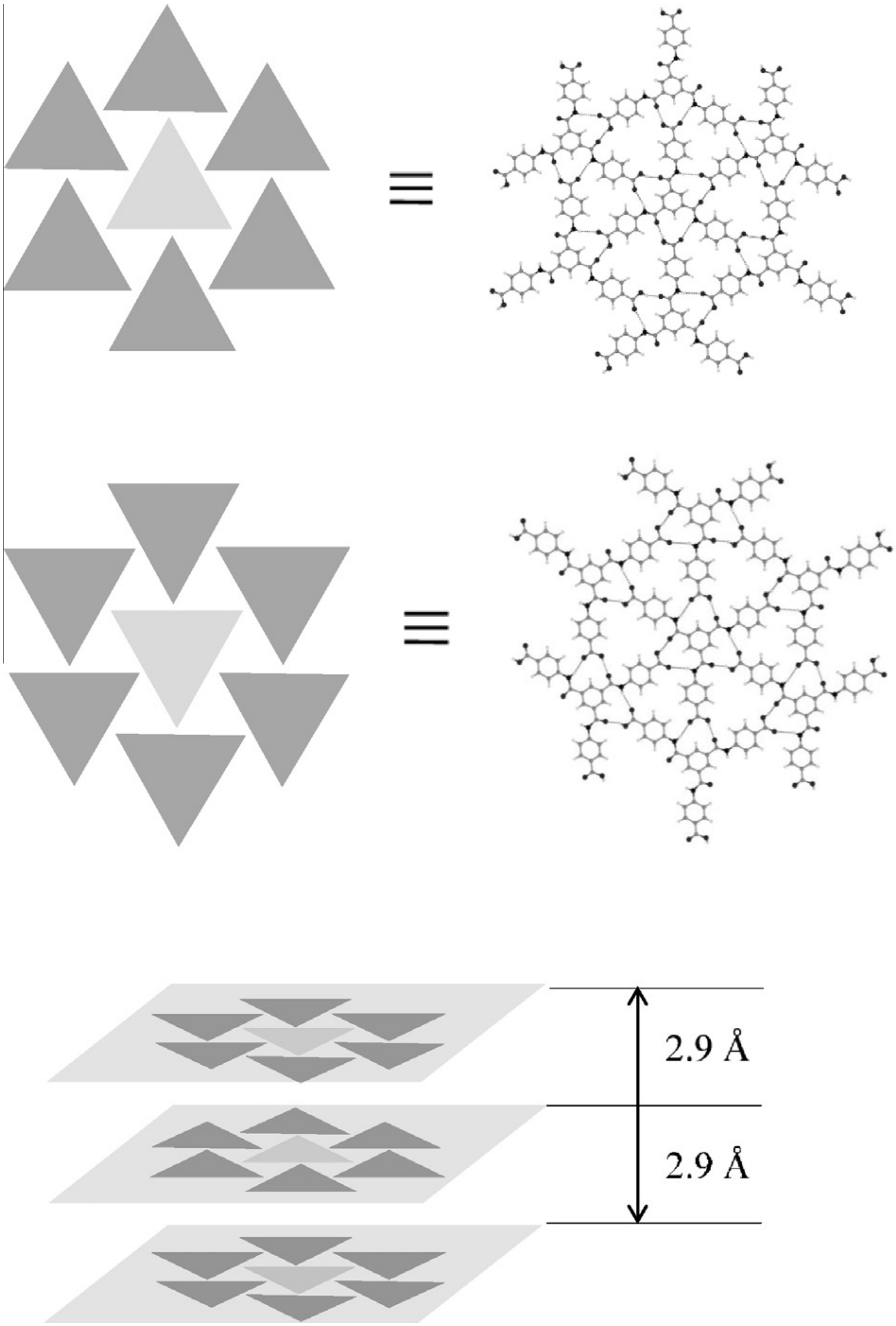

Fig. 2. A side view of the crystal structure of H_3L showing coplanar layers in the lattice.

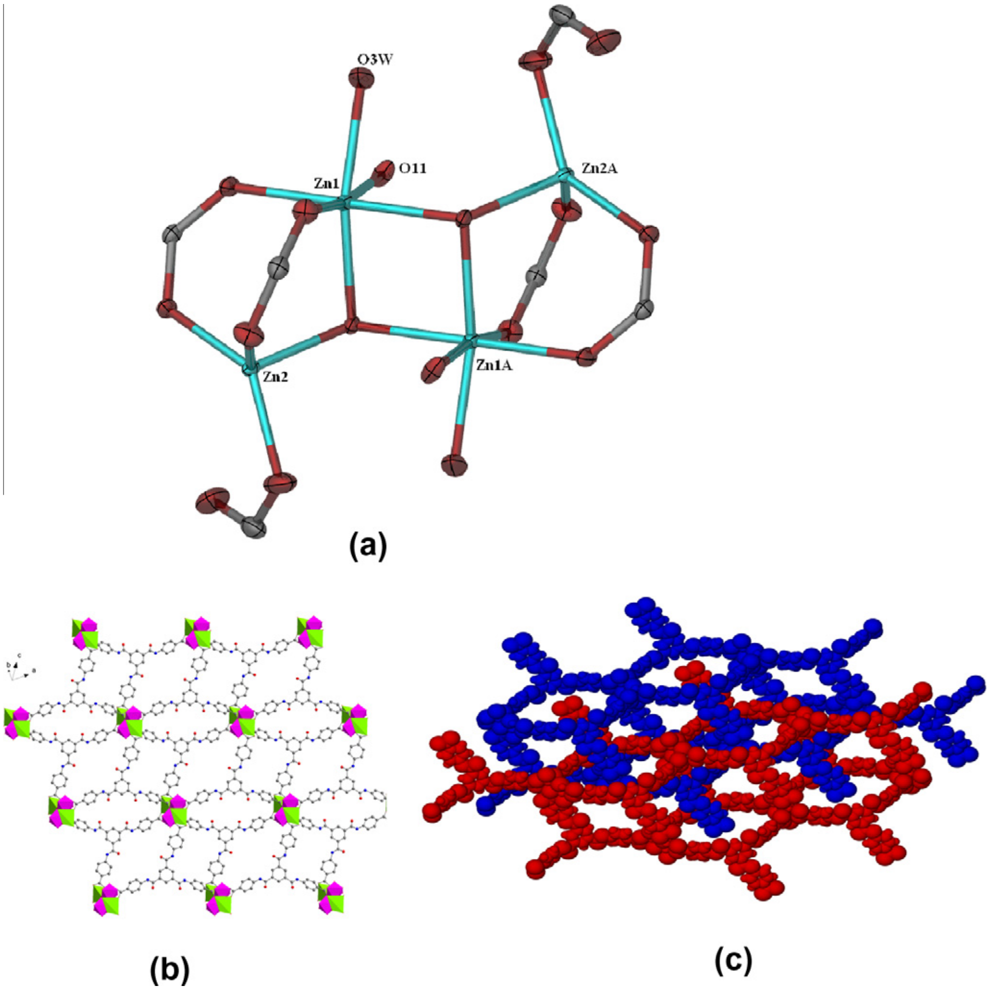

Fig. 3. (a) Coordination environment of tetranuclear $Zn_4(\mu_3\text{-}OH)_2(COO)_6(H_2O)(DMF)$ core drawn at 30% probability in **1**. Symmetry code: A: $-x+2, -y-1, -z+1$. (b) Layer structure of **1** with the Zn^{2+} atoms are shown in polyhedral mode (purple octahedron: Zn1 and Zn1a; green tetrahedron: Zn2 and Zn2a). (c) doubly-interpenetrated framework of **1**. (Colour online.)

water molecules. The layered structure is composed of tetragon-sharing edges or vertexes, corresponding to a CdI_2-type architecture, which is quite rare in organic–inorganic hybrid materials [21]. Due to the existence of large grilles, independent equivalent frameworks further interpenetrated to give a twofold interpenetrated architecture as shown in Fig. 3c.

3.1.3. Crystal structure of $[Co_3(L)_2(DMF)(H_2O)]\cdot DMF\cdot 3CH_3OH$ (**2**)

Single-crystal diffraction study revealed that **2** possesses a twofold interpenetrating three-dimensional architecture. The asymmetric unit consists of three cobalt ions, two L^{3-} ligands, one μ_3-O atom, and one coordinated DMF molecule. The three cobalt atoms in the asymmetric unit are bridged by one μ_3-O and six carboxylate groups to form a trimeric SBU $[Co_3(COO)_6(H_2O)(DMF)]$ (Fig. 4a). In this SBU, Co1 is found to adopt a tetrahedral coordination environment involving three oxygen atoms from three different carboxylate groups and one μ_3-O. Co2 is six-coordinated with a distorted octahedral geometry, and the metal center is surrounded by four oxygen atoms from four carboxylate groups, one μ_3-O, and one DMF oxygen atom. Similar to Co2, Co3 is also six-coordinated and adopts an octahedral coordination geometry completed by four oxygen atoms from three different carboxylate groups, one μ_3-O and one aqua ligand. In the trinuclear cobalt cluster, the bond distance of Co2-μ_3-O (2.091 Å) is slightly longer than that of Co1-μ_3-O (1.961 Å) and Co3-μ_3-O (1.981 Å). Trinuclear carboxylate clusters, $[M_3O(COO)_6]$, in which M represents trivalent metal ions (Al^{3+}, Cr^{3+}, Fe^{3+}), have been previously employed as SBUs for the construction of coordination polymers. However, trimeric carboxylate clusters with divalent metal ions are not common SBUs in assembling coordination polymers [22].

In the asymmetric unit, the two independent L^{3-} (labeled as L^{3-}-I and L^{3-}-II) ligands are aligned in a V-shape. The dihedral angle between the central phenyl rings of the two ligands is 20.2° and the distance is 7.084 Å, indicating no significant π-π stacking interaction exists. Each SBU connects three ligands of L^{3-}-I type and each L^3-I type ligand further connects three neighboring SBUs to form a honeycomb structure (Fig. 4b). Similar honeycomb layered structure is formed by Co_3 SBUs and ligand type of L^{3-}-II. The V-shape arrangement of ligands is responsible for the generation of the three-dimensional architecture containing large channels (19.393 × 19.622 Å in the [1 0 0] direction, 9.596 × 34.922 Å in the [0 1 0] direction). Due to the existence of large channels, interpenetration occurs between two sets of 3D network, resulting in the final twofold interpenetrating framework structure (Fig. 4d). The network has a solvent-accessible volume of 51.3%, as calculated by PLATON suite [15]. Complex **2** lacks thermal stability due to the easy loss of the coordinated DMF and water molecules at elevated temperatures. In topology, the framework of **2** can be simplified as (3,6)-network when one SBU connects six linkers and one linker joins three SBUs.

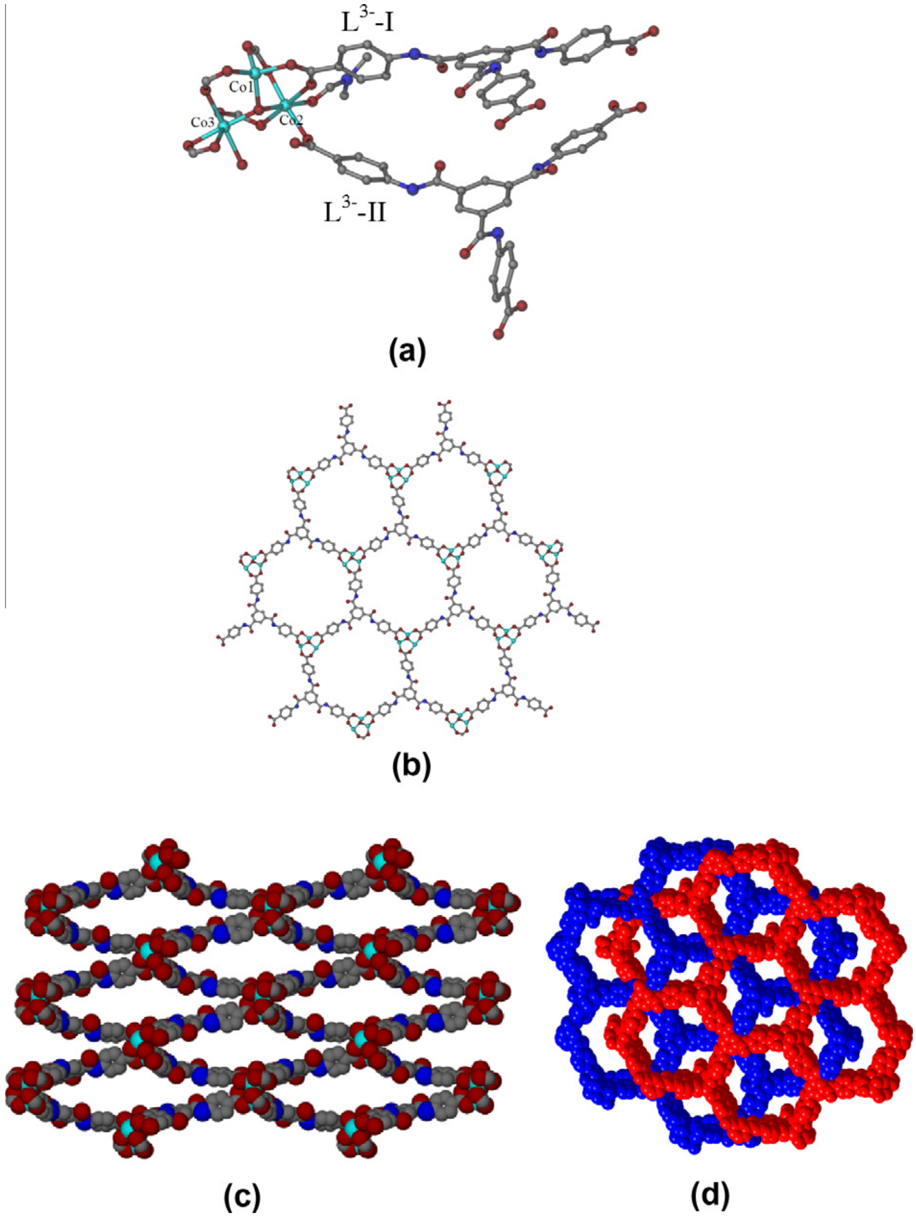

(a)

(b)

(c)

(d)

Fig. 4. (a) Coordination environment surrounding Co^{2+} atoms in $[Co_3O(L)_2(DMF)(H_2O)]\cdot DMF\cdot 3CH_3OH$ (**2**). (b) Two-dimensional honeycomb layer structure of **2** generated from connection of tricobalt atoms and L^{3-}-I/L^{3-}-II; (c) Spacing-filling showing of the three-dimensional framework of complex **2** viewed along the *b* direction; (d) Twofold interpenetrating network of **2** viewed along the *a* direction.

3.1.4. Crystal structures of $[Co_{1.5}(L)(H_2O)(DMF)]\cdot DMF$ (3) and $[Cd_{1.5}(L)(H_2O)(DMF)]\cdot DMF$ (4)

Solvothermal reaction of H_3L and $Co(NO_3)_2$ or $Cd(NO_3)_2$ in DMF/H_2O resulted in the formation of complex **3** or **4**. X-ray analysis showed that complexes **3** and **4** are isomorphous and both crystallize in triclinic space group $P\bar{1}$. The following discussion on the structural aspect will mainly focus on complex **3**. The crystal structure of **3** exhibits a neutral, two-dimensional framework generated from linkage of trimeric cobalt clusters via L^{3-} bridges. Such linear Co_3 unit is composed of two kinds of cobalt atoms. One (Co1) is octahedrally coordinated by four oxygen atoms from four different carboxylate groups and two aqua ligands. The other (Co2) and its symmetry-related (Co2A) adopt a distorted [O6] coordination geometry with five oxygen atoms from three different carboxylate groups and one oxygen atom from DMF molecule. In all, one Co1 and two Co2 are bridged by six carboxylate groups to form a linear $Co_3(CO_2)_6$ trimeric cluster in **3** (Fig. 5a). It is noteworthy that this linear SBU is also rare in cobalt coordination compound [22,23].

The three benzoate units in L^{3-} can be divided into two groups. Two carbonyl groups of the amide residues placed on the same side are named as ***A*** and the third one is ***C***. Each Co_3 core is doubly-bridged by L^{3-} ligands to form one-dimensional chain via the ***A*** part of the trinodal L^{3-} with bond types Co1–O1 2.047(3) Å, Co1–O5 2.173(4) Å, Co2–O2 2.025(4) Å, Co2–O4 2.211(4) Å, Co2–O5 2.230(3) Å, as shown in Fig. 5b. Significant hydrogen bonding of N–H···O type exists among the bridging ligands. Another noteworthy characteristic of **3** is the existence of intermolecular π–π stacking interactions, as the centroid–centroid distances between the central phenyl rings belonging to adjacent L^{3-} moieties are 3.452 Å, which fall within the normal range of π–π stacking interactions. The dihedral angles between the corresponding phenyl groups are 0°, suggesting that they are parallel to each other (Fig. 5b). The third part ***C*** further pillars the chains to form a layer.

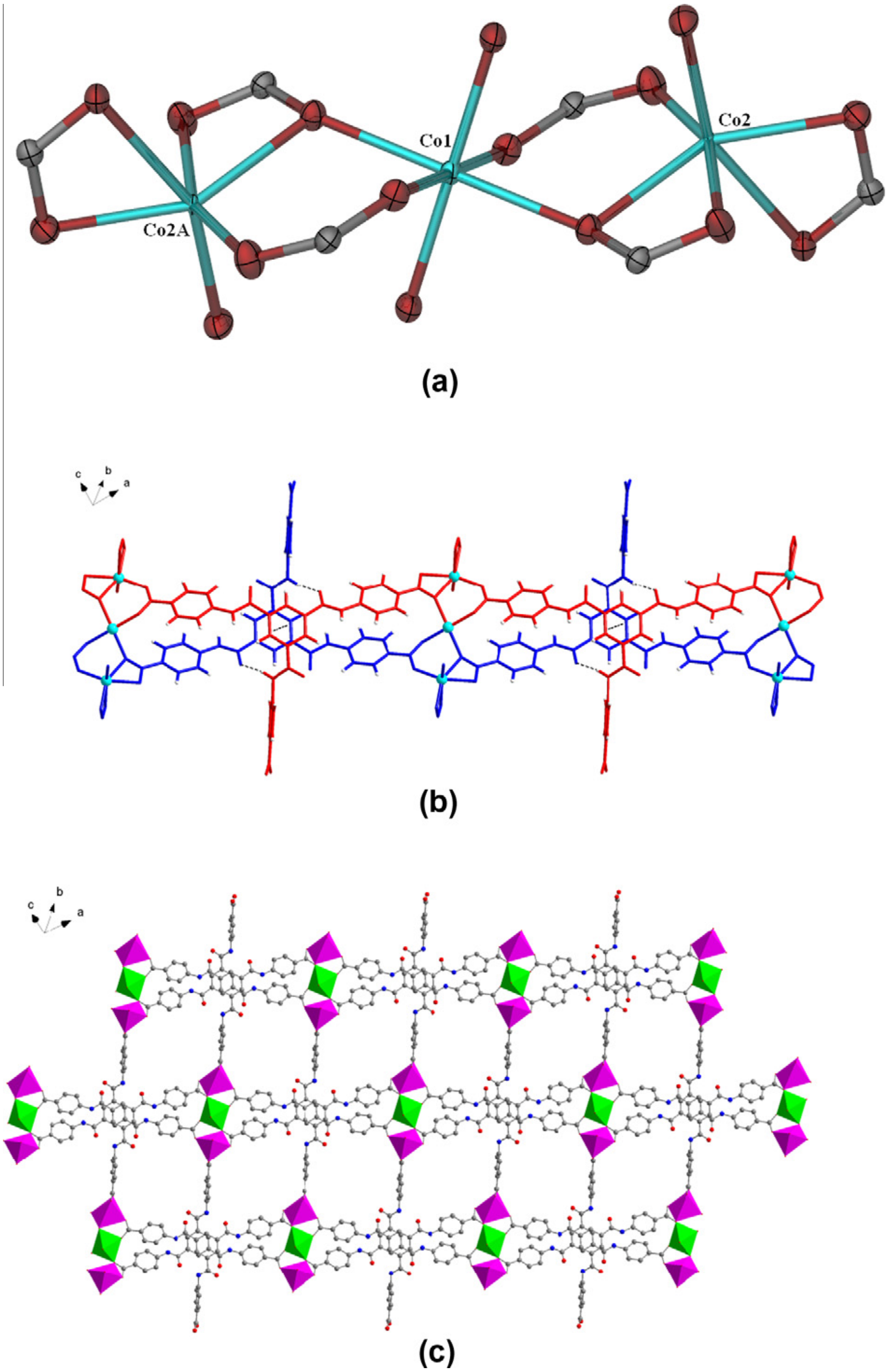

Fig. 5. (a) Coordination environment of the trinuclear $Co_3(\mu_3\text{-}O)(COO)_6(DMF)(H_2O)$ SBU in $[Co_{1.5}(L)(H_2O)(DMF)]\cdot DMF$ (**3**). Symmetry code: A: *x*, *y* + 1, *z*. (b) The hydrogen-bonding and π–π stacking interactions between the doubly-bridging ligands $N_2–H_2B\cdots O_6$ = 153°, $N_2\cdots O_6$ = 2.865(6) Å]. (c) Polyhedral representation of the two-dimensional (4,4)-network based on the linear SBUs, indicating the pore of about 11.0 × 9.24 Å (purple octahedron: Co2 and Co2A; green octahedron: Co1). (Colour online.)

Topological analysis suggests that the framework of **3** can be described as (4,4)-net layer (Fig. 5c).

To verify our initial design strategy, C_3-symmetric H_3L (Fig. 6a) ligand was employed. Several different conformations of L^{3-} have been found upon its interaction with metal ions (Fig. 6b–e, Table 2). When interacts with metal ions, it undergoes distortion and the C_3 symmetry was reduced. In both **1** and **3**, the two carbonyl groups of the amide residues are placed on the same side. The trigonal angles of the ligands are in the range of 92.21(6)–132.98(6)° and 92.26(6)–145.04(7)°, respectively. In complex **2**, trigonal angles of the two independent L^{3-} ligands in the asymmetric unit are in the range of 117.04(6)–120.40(6)° and 113.62(8)–120.4(7)°, respectively. It can then be concluded that the overall conformation of the ligand in different coordination polymers varies depending on the coordination environments in the framework.

3.2. Thermogravimetric and PXRD

Thermogravimetric analyses (TGA) are performed on crystalline samples to examine the thermal stability. As shown in Fig. S1, complex **1** exhibits a large weight loss (21.8%) at 100–200 °C, corresponding to the loss of all the water and DMF molecules in the

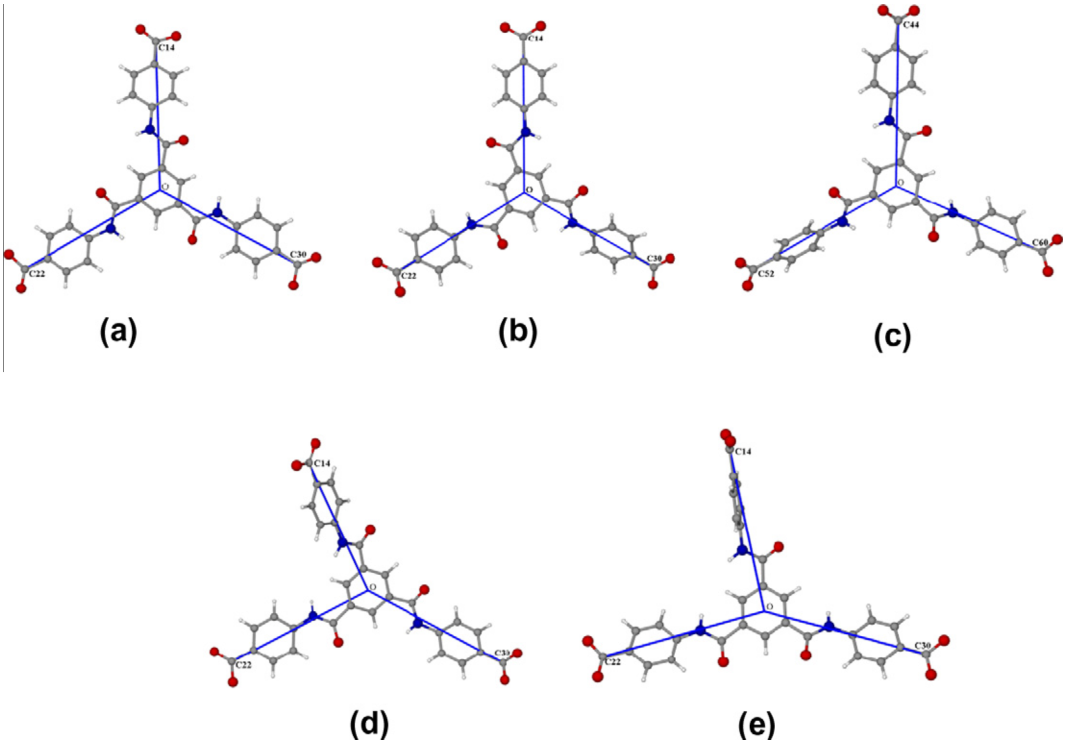

Fig. 6. Conformations of 4,4′,4″-[1,3,5-Benzenetriyltris(carbonylimino)]trisbenzoic units in (a) H_3L; (b) complex **2**; (c and d) complex **3** and (e) complex **4**. The trigonal angle was measured from the C atom of the carboxylic group to the dummy atom, the center of the central phenyl ring of the ligand, to another C atom of a neighboring carboxylic group in the ligand.

structure (Calc., 20.4%). Decomposition of **1** begins at 250 °C. Judging from the TGA curve of complex **2** (Fig. S2), all the guest molecules are lost in the temperature range of 50–250 °C (17.1%), which corresponds to one DMF and three CH_3OH molecules (Calc., 16.5%). So it is reasonable to give **2** with formula $[Co_3(L)_2(DMF)(H_2O)]\cdot DMF\cdot 3CH_3OH$. The TGA curves of **3** and **4** are similar, with the weight loss of 19.8% and 17.6% in the range of 100–260 °C, respectively, which are consistent with the calculated weight loss of all guest molecules (Calc., 20.0% for **3** and 18.3% for **4**) (Fig. S3).

PXRD analyses are carried out to check the structural identity. For each compound, the measured PXRD pattern closely matches the one simulated from single-crystal diffraction data, indicating the phase purity (Figs. S4–S7). Comparison of the PXRD patterns of the **3** and **4** further proved they are isomorphous.

4. Conclusions

In summary, a C_3-symmetric ligand H_3L has been utilized to assemble core-rosette structure and coordination polymers under solvothermal conditions. The core-rosette structure was generated by hydrogen-bonding interactions between the carboxylic acid units and amide groups. Reactions of the ligand with Zn^{2+}, Co^{2+} and Cd^{2+} resulted in the formation of coordination polymers **1**, **2**, **3** and **4**. Complex **1** presents a CdI_2-type layer structure with a SBU of $Zn_4(\mu_3\text{-}OH)_2(COO)_6(H_2O)(DMF)$ containing both 4- and 6-coordinated Zn^{2+}. Complex **2** was found to possess a doubly-interpenetrated three-dimensional network with a SBU of $[Co_3(COO)_6(H_2O)(DMF)]$ cluster. The linear $Co_3(CO_2)_6$ trimeric cluster in **3** is rarely observed in cobalt coordination compounds. These results proved that H_3L is a useful and intriguing ligand in the construction of coordination polymers or frameworks. Further investigations of the structural diversity of H_3L-derived metal complexes and their applications in catalysis and gas storage are in progress.

Acknowledgments

The authors gratefully acknowledge the National Natural Science Foundation of China (NSFC No. 20801018), Shanghai education development foundation for financial support (Grant No. 2008CG31) and Shanghai Rising-Star Program (10QA1402000). We also acknowledge financial support by The Open University of HongKong (Project No. 10/1.1).

Appendix A. Supplementary data

CCDC 805020, 805021, 805022, 805023 and 808033 contains the supplementary crystallographic data for H_3L, complex **1**, **3**, **4** and **2**. These data can be obtained free of charge via http://www.ccdc.cam.ac.uk/conts/retrieving.html, or from the Cambridge Crystallographic Data Centre, 12 Union Road, Cambridge CB2 1EZ, UK; fax: (+44) 1223 336 033; or e-mail: deposit@ccdc.cam.ac.uk. Supplementary data associated with this article can be found, in the online version, at doi:10.1016/j.poly.2011.11.010.

References

[1] (a) W.B. Lin, J. Solid State Chem. 178 (2005) 2486;
(b) J.S. Seo, D. Whang, H. Lee, S.I. Jun, J. Oh, J. Young, K. Kim, Nature 404 (2000) 982;
(c) R. Zou, H. Sakurai, Q. Xu, Angew. Chem., Int. Ed. 45 (2006) 2542.
[2] (a) O. Sato, Acc. Chem. Res. 36 (2003) 692;
(b) E.Q. Gao, F. Yue, S.Q. Bai, Z. He, C.H. Yan, J. Am. Chem. Soc. 126 (2004) 1419; X.Y. Wang, X.Y. Wang, S. Gao, Chem. Commun. (2008) 281.
[3] (a) P. Horcajada, C. Serre, M. Vallet-Regí, M. Sebban, F. Taulelle, G. Férey, Angew. Chem., Int. Ed. 45 (2006) 5974;
(b) P. Horcajada, C. Serre, G. Maurin, N.A. Ramsahye, F. Balas, G. Férey, J. Am. Chem. Soc. 130 (2008) 6774.
[4] (a) S.Q. Ma, D.F. Sun, X.S. Wang, H.-C. Zhou, Angew. Chem., Int. Ed. 46 (2007) 2458;
(b) J.L.C. Rowsell, O.M. Yaghi, Angew. Chem., Int. Ed. 44 (2005) 4670;

(c) B. Chen, M. Eddaoudi, S.T. Hyde, M. O'Keeffe, O.M. Yaghi, Science 291 (2001) 1021.

[5] S. Noro, S. Kitagawa, M. Yamashita, T. Wada, Chem. Commun. (2002) 222;
(b) R. Kitaura, G. Onoyama, H. Sakamoto, R. Matsuda, S. Noro, S. Kitagawa, Angew. Chem., Int. Ed. 43 (2004) 2684;
(c) B. Chen, F.R. Fronczek, A.W. Maverick, Inorg. Chem. 43 (2004) 8209;
(d) P.A. Maggard, B. Yan, J. Luo, Angew. Chem., Int. Ed. 44 (2005) 2;
(e) B. Chen, N.W. Ockwig, A.R. Millward, D.S. Contreras, O.M. Yaghi, Angew. Chem., Int. Ed. 44 (2005) 4745;
S.H. Cho, B. Ma, S.T. Nguyen, J.T. Hupp, T.E. Albrecht-Schmitt, Chem. Commun. (2006) 2563.

[6] (a) J.S. Seo, D. Whang, H. Lee, S.I. Jun, J. Oh, Y.J. Jeon, K. Kim, Nature 404 (2000) 982;
(b) R. Kitaura, K. Fujimoto, S. Noro, M. Kondo, S. Kitagawa, Angew. Chem., Int. Ed. 41 (2002) 4745;
(c) D.M. Shin, I.S. Lee, Y.K. Chung, Inorg. Chem. 42 (2003) 8838;
(d) R. Custelcean, M.G. Gorbunova, J. Am. Chem. Soc. 127 (2005) 16362.

[7] Y. Zou, M. Park, S. Hong, M.S. Lah, Chem. Commun. (2008) 2340;
X. Song, Y. Zou, X. Liu, M. Oha, M.S. Lah, New J. Chem. 34 (2010) 2396;
(c) M.J. Prakash, Y. Zou, S. Hong, M. Park, M.-P.N. Bui, G.H. Seong, M.S. Lah, Inorg. Chem. 48 (2009) 1281.

[8] (a) S. Ma, H.-C. Zhou, J. Am. Chem. Soc. 128 (2006) 11734;
D. Sun, Y. Ke, T.M. Mattox, A.O. Betty, H.-C. Zhou, Chem. Commun. (2006) 5447;
(c) S. Ma, X.-S. Wang, D. Yuan, H.-C. Zhou, Angew. Chem., Int. Ed. 47 (2008) 1;
(d) X.-S. Wang, S. Ma, D. Sun, S. Parkin, H.-C. Zhou, J. Am. Chem. Soc. 128 (2006) 16474;
(e) D. Sun, S. Ma, Y. Ke, D.J. Collins, H.-C. Zhou, J. Am. Chem. Soc. 128 (2006) 3896.

[9] S. Hasegawa, S. Horike, R. Matsuda, S. Furukawa, K. Mochizuki, Y. Kinoshita, S. Kitagawa, J. Am. Chem. Soc. 129 (2007) 2607.

[10] B. Zheng, J. Bai, J. Duan, L. Wojtas, M.J. Zaworotko, J. Am. Chem. Soc. 133 (2011) 2607.

[11] (a) B.D. Hosangdi, R.H. Dave, Tetrahedron Lett. 37 (1996) 6375;
(b) M.C. Davis, Synth. Commun. 37 (2007) 1457.

[12] Bruker, SMART 5.0 and SAINT 4.0 for Windows NT, Area Detector Control and Integration Software. Bruker Analytical X-ray Systems Inc., Madison, WI, 1998.

[13] G.M. Sheldrick, SADABS: Program for Empirical Absorption Correction of Area Detector Data; University of Göttingen, Göttingen, Germany, 1996.

[14] G.M. Sheldrick, SHELXTL 5.1 for Windows NT: Structure Determination Software Programs; Bruker Analytical X-ray Systems Inc., Madison, WI, 1997.

[15] A.L. Spek, PLATON, A Multipurpose Crystallographic Tool, Utrecht University, Utrecht, The Netherlands, 2001.

[16] (a) S. Vázquez-Campos, M. Péter, M.-D. Dong, S.-L. Xu, W. Xu, H. Gersen, T.R. Linderoth, H. Schönherr, F. Besenbacher, M. Crego-Calama, D.-N. Reinhoudt, Langmuir 23 (2007) 10294;
(b) P. Jonkheijm, A. Miura, M. Zdanowska, F.J.M. Hoeben, S. De Feyter, A.P.H.J. Schenning, F.C. De Schryver, E.W. Meijer, Angew. Chem., Int. Ed. 43 (2004) 74;
(c) S. Yagai, T. Nakajima, T. Karatsu, K. Saitow, A. Kitamura, J. Am. Chem. Soc. 126 (2004) 11500;
(d) J.M. Kerckhoffs, T. Ishi-i, V. Paraschiv, P. Timmerman, M. Crego-Calama, S. Shinkai, D.N. Reinhoudt, Org. Biomol. Chem. 1 (2003) 2596;
(e) C. Thalacker, F. Würthner, Adv. Funct. Mater. 12 (2002) 209;
(f) H. Fenniri, B.-L. Deng, A.E.J. Ribbe, J. Am. Chem. Soc. 124 (2002) 11064;
(g) J. Lu, Q.-D. Zeng, C. Wang, Q.-Y. Zheng, L.-J. Wan, C.-L. Bai, J. Mater. Chem. 12 (2002) 2856;
(h) A. Nangia, Curr. Opin. Solid State Mater. Sci. 5 (2001) 115;
(i) S. Valiyaveettil, K. Mülllen, New J. Chem. (1998) 89.

[17] (a) J. Han, C.-W. Yau, C.-K. Lam, T.C.W. Mak, J. Am. Chem. Soc. 130 (2008) 10315;
(b) C.-K. Lam, F. Xue, J.-P. Zhang, X.-M. Chen, T.C.W. Mak, J. Am. Chem. Soc. 127 (2005) 11536;
(c) T.C.W. Mak, C.-K. Lam, J. Han, Q. Li, F. Xue, Urea/thiourea/selenourea-anion host lattices stabilization of labile species and designed constrction of rosette ribbons and layers, in: E.R.T. Tiekink, J.J. Vittal, M.J. Zaworotko (Eds.), Organic Crystal Engineering, Wiley, Chichester, 2010, pp. 239–312 (Chapter 8).

[18] R. Liu, K.-F. Mok, S. Valiyaveettil, New J. Chem. 25 (2001) 890.

[19] D. Sun, Y. Ke, T.M. Mattox, S. Parkin, H.-C. Zhou, Inorg. Chem. 45 (2006) 7566.

[20] (a) M. Eddaoudi, J. Kim, N. Rosi, D. Vodak, J. Wachter, M. O'Keeffe, O.M. Yaghi, Science 295 (2002) 469;
(b) U. Mueller, M. Schubert, F. Teich, H. Puetter, K. Chierle-Arndt, J. Aster, J. Mater. Chem. 16 (2006) 626.

[21] T. Devic, M. Evain, Y. Moelo, E. Canadell, P. Auban-Senzier, M. Fourmigue, P. Batail, J. Am. Chem. Soc. 125 (2003) 3295.

[22] L.-F. Ma, Y.-Y. Wang, L.-Y. Wang, D.-H. Lu, S.R. Batten, J.-G. Wang, Cryst. Growth Des. 9 (2009) 2036.

[23] N. Rosi, J. Kim, M. Eddaoudi, B. Chen, M. O'Keeffe, O.M. Yaghi, Science 127 (2005) 1504.